

Nanoscale

Accepted Manuscript



This is an *Accepted Manuscript*, which has been through the Royal Society of Chemistry peer review process and has been accepted for publication.

Accepted Manuscripts are published online shortly after acceptance, before technical editing, formatting and proof reading. Using this free service, authors can make their results available to the community, in citable form, before we publish the edited article. We will replace this *Accepted Manuscript* with the edited and formatted *Advance Article* as soon as it is available.

You can find more information about *Accepted Manuscripts* in the [Information for Authors](#).

Please note that technical editing may introduce minor changes to the text and/or graphics, which may alter content. The journal's standard [Terms & Conditions](#) and the [Ethical guidelines](#) still apply. In no event shall the Royal Society of Chemistry be held responsible for any errors or omissions in this *Accepted Manuscript* or any consequences arising from the use of any information it contains.

ARTICLE

Graphene quantum dots, graphene oxide, carbon quantum dots and graphite nanocrystals in coals

Cite this: DOI: 10.1039/x0xx00000x

Yongqiang Dong, Jianpeng Lin, Yingmei Chen, Fengfu Fu, Yuwu Chi* and Guonan Chen

Received 00th January 2012,
Accepted 00th January 2012

DOI: 10.1039/x0xx00000x

www.rsc.org/

Six coal samples of different ranks have been used to prepare single-layer graphene quantum dots (S-GQDs). After a chemical oxidation and a serial of centrifugation separation, every coal could be treated into two fractions, namely Coal_A and Coal_B. According to the characterization results of TEM, AFM, XRD, Raman and FTIR, Coal_A was revealed to be mainly composed of S-GQDs, which have an average height of about 0.5 nm and an average plane dimension of about 10 nm. The obtained S-GQDs showed excitation-dependent fluorescence and excellent electrochemiluminescence. Coal_B were found to be some other carbon-based nanomaterials (CNMs) including agglomerate GQDs, graphene oxide, carbon quantum dots and agglomerate carbon nanocrystals can also be found. Generally, low rank coals might be more suitable for the preparation of S-GQDs. The production yield of S-GQDs from the six investigated coals decreased from 56.30% to 14.66% when the coal rank increased gradually. In contrary, high rank coals had high production yield of Coal_B, and might be more suitable for preparing other CNMs that contained in Coal_B, although those CNMs were difficult to be separated from each other in our experiment.

Introduction

Since the discovery of fullerene and carbon nanotube (CNT),^{1,2} carbon-based nanomaterials (CNMs) have attracted significant attention for many years due to their unique optical, electrical, thermal and mechanical properties.³⁻⁴ More and more new CNMs have been found and studied. Graphene oxide (GO) is a recently exciting material,⁵ which is an atomically thin sheet of graphite that covalently decorated with abundant oxygen-containing groups, either on the basal plane or at the edges. GO has been reported to have some unique optical properties, such as fluorescence (FL) and electrochemiluminescence (ECL).⁶⁻⁸ Furthermore, GO is the most important precursor to prepare graphene, which has been widely applied in broad fields due to the low mass density, excellent electrical conductivity and high specific surface area. Up to now, GO is mainly synthesized by chemically exfoliating graphite according to modified Hummer's methods.⁹⁻¹⁰ However, the dangerous and violent chemical reaction, the boring and long-time washing procedure involved in the methods have limited seriously the large-scale preparation of GO.

Carbon-based dots (CDs) are another newly emerging CNMs, mainly including carbon nanoparticles of less than 10 nm in particle size (so-called carbon quantum dots, CQDs),¹¹ and graphene nanosheets with a plane size less than 100 nm (so-called graphene quantum dots, GQDs).¹² CDs usually exhibit fascinating optical and electro-optical properties due to the quantum confinement and edge effects.¹³⁻¹⁵ Accordingly, CDs are proposed to be promising alternatives for conventional semiconductor-based quantum dots (QDs). Compared with QDs, CDs show many outstanding advantages, such as low cost, low toxicity, robust optical/chemical inertness and easy of fabrication. CDs have been expected to have great potential applications in various fields including bio-imaging, cell-imaging, sensing, photovoltaic devices and catalysis.¹³⁻¹⁷ Therefore, growing attention has been focused on the synthesis of

CDs. Up to now, many simple and efficient methods have been proposed to synthesize kinds of CDs. These methods can be generally classified into "bottom-up" and "top-down". The "bottom-up" strategies mean carbonizing some special organic precursors (such as citric acid,^{18,19} carbohydrate,²⁰⁻²² some aromatic organics,^{23,24} or some vegetations^{25,26}) through hydrothermal,^{18,25,26} thermal,^{19,23,24} microwave,²⁰ concentration H₂SO₄,²¹ or sonication treatments.²² Usually, those "bottom-up" strategies provide advantages such as precise controlling over the morphology and the size distribution of the product,^{23,24} convenient for surface-passivation or heteroatoms doping to prepare high yield luminescent CDs.^{18,20} "Top-down" techniques are cutting some big-size carbon sources (such as graphite,^{11,27} graphene or GO,²⁸⁻³⁰ carbon nanotubes,^{27,31} activated carbon,³² carbon fibers,³³ carbon black³⁴) by chemical oxidation,³²⁻³⁴ electrochemical oxidation,²⁸ hydrothermal (or solvothermal) treatment,^{29,30} or proton ablation.¹¹ The top-down ways, especially the chemical oxidation methods, may have an advantage in producing CDs in large-scale. However, most reported precursors used in both "bottom-up" and "top-down" methods are either too expensive or difficult to be obtained, and are not suit for the mass production of CDs.

Coal, a fossil fuel, is apparently the cheapest and most abundant carbon source in the world. Recent research results indicated that coal might contain some regions or clusters that are graphite-like in nature. It seems hopeful that the graphite-like clusters could be released and separated from coals through some simple treatments, such as chemical oxidation and centrifugation. It would be great significant if some important CNMs, such as GO and CDs could be finally obtained from coal, and even better if some other CNMs could be also prepared from coal.

In the present work, six coal samples of different ranks (carbon content in raw coal sample) were systematically studied. After a chemical oxidation and a serial of centrifugation separations, high yield single-layer graphene quantum dots (S-GQDs) with

good FL and excellent ECL properties were finally obtained from all coal samples. The production yield of S-GQDs was revealed to be dependent on the rank of coal. In the six investigated coals, the production yield of S-GQDs decreases from 56.30% to 14.66% when the carbon content increases from 66.36% to 90.20%. That is to say, low rank coals may be more suitable than high rank coals to prepare S-GQDs. Besides S-GQDs, many other CNMs including agglomerate GQDs, GO, CQDs and agglomerate carbon nanocrystals were also found in the coals. Although, the other CNMs are not able to be separated from coal in our experiment, coal should be also a potential source of those materials. This study is of significance for not only the preparation of GQDs, but also other CNMs, such as graphene and CQDs.

Experimental

Materials

Six coal samples with different carbon contents were selected in this study (Table S1). All coal samples were ground to pass a 200-mesh screen (i.e. diameter of particles less than 0.74 mm) and dried before experiment. Other chemicals were analytically pure and used as received. Doubly distilled water was used throughout the experiments.

Instrumentation

Elemental analysis was carried out using a Vario MICRO organic elemental analyzer. Fourier transform infrared (FT-IR) spectra were recorded on a Thermo Nicolet 360 spectrophotometer. X-ray photoelectron spectroscopy (XPS) spectra of C 1s were measured by a ESCALab 250 XPS system having an Al K source for determining the composition and chemical bonding configurations. X-ray powder diffraction (XRD) patterns were obtained from a Japan Rigaku D/max-3C using Cu K radiation. Raman spectra were measured using a Renishaw 1000 microspectrometer (excitation wavelength of 514.5 nm). High resolution transmission electron microscopy (HRTEM) measurements were performed on a Tecnai G2 F20S-TWIN electronic microscope at operation voltage of 200 KV. The height distribution of the obtained GQDs was characterized by atomic force microscopy (AFM) (Nanoman, Veeco, Santa Barbara, CA) by using tapping mode. UV-Vis absorption spectra were recorded by a Lambda 750 UV/Vis spectrophotometer. All fluorescent (FL) spectra were obtained by a Cary Eclipse Varian fluorescence spectrophotometer. Electrochemiluminescent (ECL) signals were measured simultaneously by an ECL & electrochemistry multi-functional detection system (MPI-E, Remex Electronic Instrument Lt. Co., Xi'an, China) equipped with a three-electrode system (a Pt wire working electrode with 0.3 cm² surface area, a Pt wire counter electrode and an Ag/AgCl reference electrode).

Preparation of CDs

The coal sample (SD) with a moderate carbon content was chosen as the example to demonstrate the preparation of CNMs. As illustrated in Fig. 1, 0.5 g dried coal sample was refluxed with 100 mL 5 mol L⁻¹ HNO₃ at 130 °C for 12 h, and the resultant suspension was cooled to room temperature with cool water. The obtained suspension was centrifuged (2770g) for 30 min to collect the supernatant and the deposit. Subsequently, both the supernatant and the deposit underwent the same

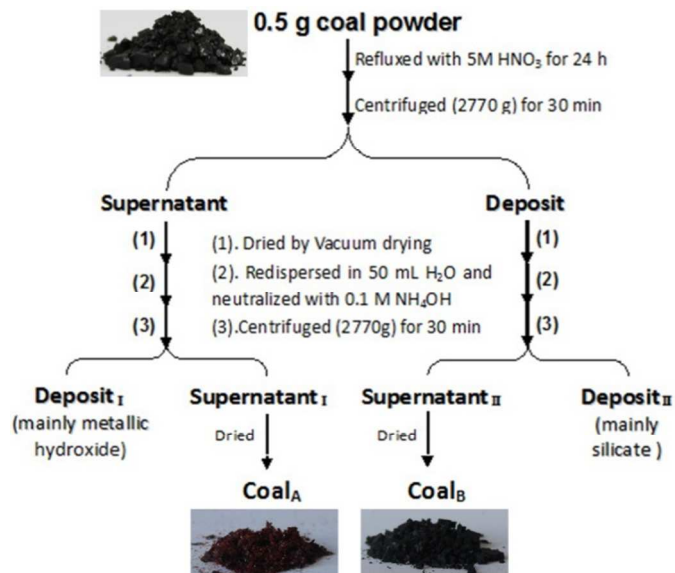


Fig. 1 Treatment procedures of coal samples.

procedures as following: 1) The supernatant (or deposit) was dried by vacuum drying. 2) The obtained solid was dispersed with 30 mL double-distilled water and subsequently neutralized with 0.1 mol L⁻¹ NH₄OH. 3) The obtained solution was centrifuged (2770g) for 30 min. After that, the supernatant was separated as Deposit (I) and Supernatant (I) while the deposit was separated as Deposit (II) and Supernatant (II). The Supernatant (I) and Supernatant (II) were dried and labeled as nitric acid-soluble fraction (Coal_A) and nitric acid-insoluble fraction (Coal_B), respectively. It should be pointed out that the suspension obtained from refluxing coal with concentrated HNO₃ must not be neutralized before the centrifugation. Otherwise, only little deposit could be obtained after the centrifugation. In other words, Coal_A and Coal_B would not be separated from each other.

Results and discussion

Elemental analysis results (Table 1) show that both Coal_A and Coal_B are composed of abundant carbon, oxygen elements, and small amounts of nitrogen, hydrogen elements. FT-IR spectra of Coal_A and Coal_B (Fig. S1) show obvious absorption peaks of C=C, C=O, C-O, O-H groups. XPS spectra show that both Coal_A and Coal_B present three main peaks associated with carbon atoms, which located at 284.5 eV (C-C sp²), 286.1 eV (C-O), and 287.8 eV (C=O) (Fig. 2a). The results of FT-IR and XPS indicate that both Coal_A and Coal_B contain abundant graphite-like structures and a lot of oxygen-containing groups (mainly carboxyl and hydroxyl groups). The graphite-like structures are further confirmed with the results of XRD and Raman studies. XRD profiles of both Coal_A and Coal_B show wide (002) peaks centred at around 25° (Fig. 2b). The Raman spectra of both Coal_A and Coal_B (Fig. 2c) show the characteristic D band at 1385 cm⁻¹ and G band at 1600 cm⁻¹. All characterization results mentioned above are similar to those of many previously reported CNMs (such as GQDs, CQDs, and

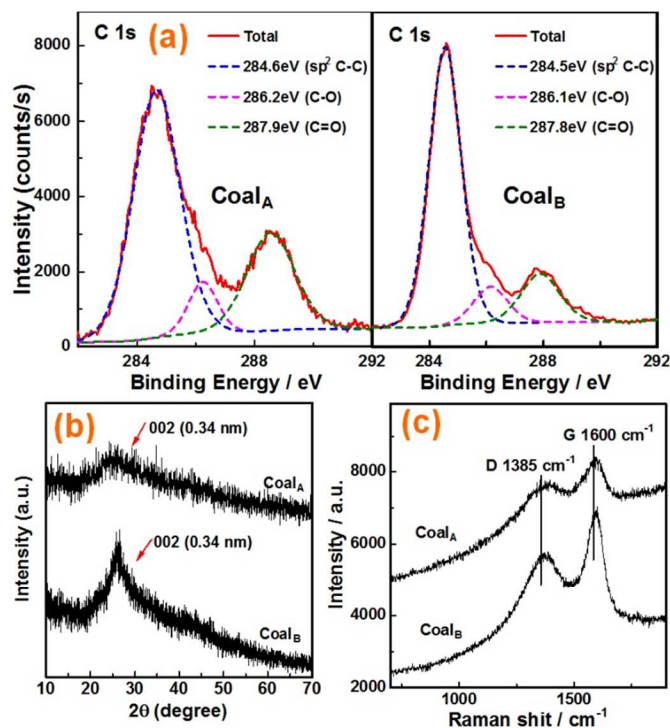


Fig. 2 XPS spectra of C 1s (a), XRD pattern (b), and Raman spectra (c) of Coal_A and Coal_B.

few-layer graphene nanoribbons). That is to say both Coal_A and Coal_B should be mainly composed of CNMs. However, there should be something different between Coal_A and Coal_B. Firstly, the carbon content of Coal_B is higher while the oxygen content is lower when compared with those of Coal_A. Secondly, Coal_B exhibits more fraction of C-C sp² in the XPS measurement. Thirdly, the XRD peak of Coal_B is much sharper than that of Coal_A. Finally, the relative intensity of the “disorder” D band to the crystalline G band (I_D/I_G) for the Coal_B is calculated to be about 0.70, which is lower than that of Coal_A (0.83). These different characteristics imply that the graphit-like structures of Coal_B should be bigger than those of Coal_A, and Coal_A should have higher “disorder” intensity.

HRTEM results indicate that Coal_A is mainly composed of nanosheets of about 10 nm in size, without any obvious lattice fringe (Fig. 3a). AFM image indicates that the height of these nanosheets is mainly distributed in the range of 0.3 to 0.9 nm, with an average value of about 0.5 nm (Fig. 3b). These results are very similar to those of single layered GQDs (S-GQDs) reported in our previous work,³⁴ suggesting that Coal_A is also mainly S-GQDs. As shown in Fig. 3c, Coal_A solution shows a broad UV-vis absorption below 480 nm, with a shoulder and a peak at around 400 and 280 nm, respectively. The FL spectra are broad, ranging from 420 (blue) to 540 nm (yellow), with a dependence of the excitation wavelengths. The pale yellow Coal_A solution shows blue luminescence under the irradiation of 365 nm UV light (the inset of Fig. 3c). The FL quantum yield of Coal_A solution at 365 nm was calculated to be about 1.8%, by selecting the quinine sulfate as standard. Besides the photoluminescence, the Coal_A solution also exhibits excellent ECL activity. When 1 Hz potential steps between +1.8 V and -1.5 V are applied, transient ECL signal resulting from electron transfer reaction between reduced and oxidized Coal_A is

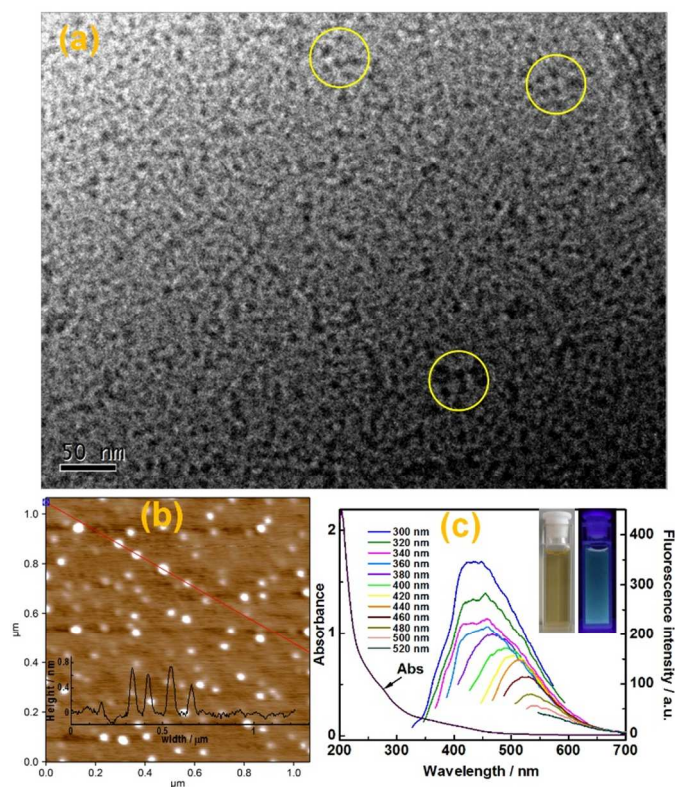


Fig. 3 (a) HRTEM, (b) AFM images and (c) UV-vis absorption and fluorescence spectra (recorded for progressively longer excitation wavelengths from 280 to 520 nm increments) of Coal_A. The inset in (b) is the height profile along the red line in (b). The insets in (c) are photographs of the Coal_A aqueous solution (0.2 mg/mL) taken under a visible light (left) and a 365 nm UV light (right).

detected in both negative and positive potential pulses (inset a in Fig. 4).³¹ When the potential is cycled between -1.5 and +1.8 V, Coal_A produces only a very weak cathodic ECL signal. However, the weak ECL signal is dramatically enhanced by S₂O₈²⁻. Furthermore, the enhanced ECL signal is very stable during a continuous potential scan (Fig. S2), indicating that Coal_A and S₂O₈²⁻ can form an excellent coreactant ECL system (Fig. 4). The ECL spectrum is in good agreement with that of S-GQDs from XC-72 carbon black (inset b in Fig. 4). All these results indicate that Coal_A is mainly composed of S-GQDs and have potential applications in many fields, especially in sensing and bioimaging.

In contrast, HRTEM images show that the microstructures of Coal_B are much more complex. Typically, at least four types of CNMs can be found from the Coal_B of sample SD. 1) Abundant thin-layer nanostructures of about 20 nm in width (Fig. 5a) and some irregular aggregates of the thin-layer nanostructures (Fig. 5b) can be easily to be found. Neither the thin-layer nanostructures nor the aggregates show any obvious lattice structure. It is supposed that the thin-layer nanostructures should be similar in nature with the S-GQDs found in the Coal_A, but bigger than the S-GQDs in width. In other words, the thin-layer nanostructures may be some intermediates between S-GQDs and graphene. 2) Some big layer-like material (Fig. 5c) can also be found in the Coal_B. As discussed above, it is unreasonable for any organic to present in Coal_B. Furthermore,

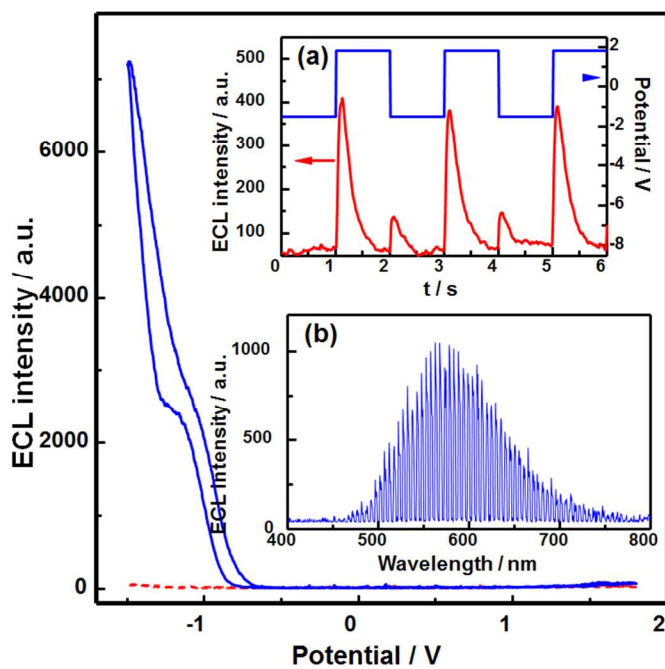


Fig. 4 ECL of the obtained 0.2 mg/mL Coal_A in 0.1M PBS solution (pH=7.0) in the presence (blue) and absence (red) of 1mM K₂S₂O₈. Inset: (a) ECL transients (lower curves) by stepping potential (upper curves) between -1.5V and +1.8V of the obtained CQDs. (b) ECL spectra of the Coal_A/S₂O₈²⁻ system and the S-GQDs/S₂O₈²⁻.

ordinary organic should not stable under the irradiation of high-energy electron-beam of TEM. Therefore, it is supposed that the observed layer-like material could be graphene (or GO). 3) Some monodisperse nanocrystals with a lattice spacing of 0.212 nm, which agrees with that of the (100) facet of graphite, can also be easily found in Coal_B. Those graphite-structured nanocrystals have a uniform spherical shape and a narrow size distribution of 3 to 5 nm, and should be so called CQDs (Fig. 5d). 4) Some big aggregates (Fig. 5e) composed of inordinate crystals are found in the Coal_B. These crystals have a lattice spacing of 0.337 nm and a lattice spacing of 0.213 nm (Fig. 5f), corresponding to those of the (002) facet and the (100) facet, respectively. Although it is difficult to be completely separated from each other in our experiment, the discovery of these kinds CNMs implies that the coal would also be a potential source to prepare these CNMs, including graphene (or GO), CQDs and carbon nanocrystals. It should be mentioned that Coal_B can also exhibit FL and ECL (Fig. S3 and Fig. S4). The FL and ECL behaviors of Coal_B are quite similar with those of Coal_A. However, the FL and ECL intensities of Coal_B are much weaker than those of Coal_A at the same mass concentration.

On the basis of the experimental results mentioned above, it can be known that Coal_A is mainly composed of small-size S-GQDs, while Coal_B is composed of some relatively big-size CNMs. Then, it is worth discussing the relationship between the coal nature and the product yields of Coal_A and Coal_B. As shown in Fig. 6, low rank coals (coal samples with low carbon content) have very high product yields of Coal_A (even as high as 56.30%). With the increase of coal rank, the production yield of Coal_A decreases whereas the production yield of Coal_B increases. In other words, low rank coals contain more fraction of small-size S-GQDs and less fraction of big-size IC than high

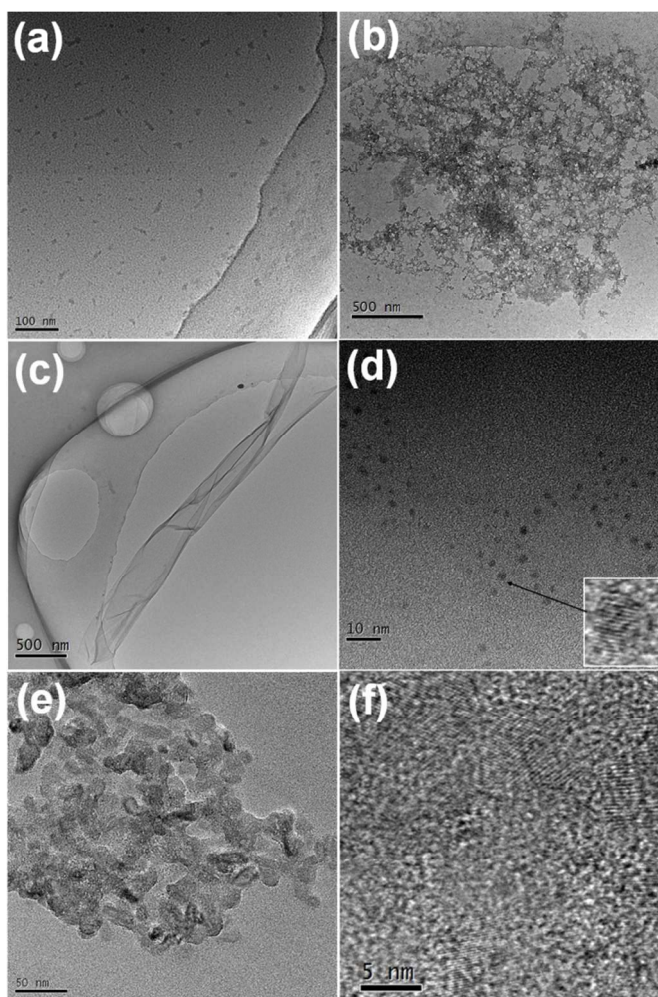


Fig. 5 HRTEM images of Coal_B: (a) thin-layer nanostructures; (b) irregular aggregates of thin-layer nanostructures; (c) graphene; (d) monodisperse CQDs; (e) and (f) big aggregates composed of inordinate carbon nanoparticles with different magnification.

rank coals. It should be pointed out that the summation of product yields of Coal_A and Coal_B may be higher than 100% in some high rank coals (such as SD, ZBM093, ZBM094). That is because the chemical oxidation has introduced abundant oxygen into both Coal_A and Coal_B.

To discuss the formation mechanisms of Coal_A and Coal_B, two control parallel control experiments were done by using graphite powder and liquid paraffin as raw materials. However, neither fraction like Coal_A nor fraction like Coal_B was obtained. The experimental results indicated that the refluxing treatment with 5 M HNO₃ could neither break down the big graphite into small-size carbon based nanomaterials nor carbonize organics into graphite-based nanomaterials. Therefore, Coal_A and Coal_B are likely to be initially present yet immobilized in those raw coal samples. After being refluxed with nitric acid, Coal_A and Coal_B are released into the aqueous phase due to carboxylation.^{32,34} Recent research results indicate that organics can be carbonized into GQDs, CQDs or graphene after thermal or hydrothermal treatments.^{19,24,35,36} Furthermore, continuous heating is helpful to convert tiny GQDs into big-size

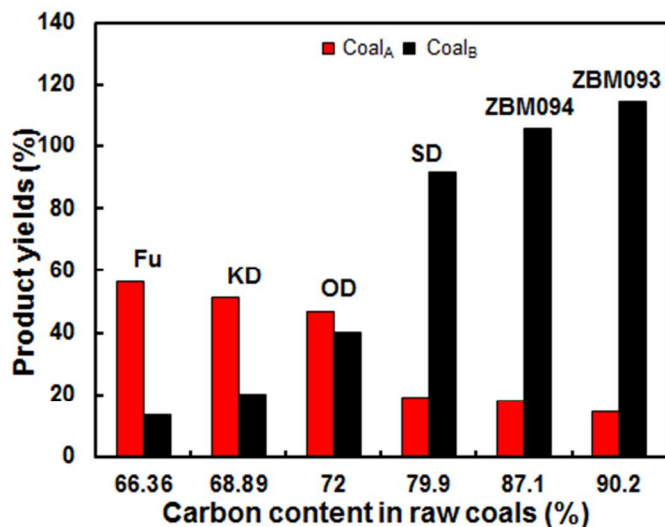


Fig. 6 Relationship between TC content of coal sample and production weight of Coal_A (blue column) and Coal_B (red column) from 0.5 g coal samples.

graphene.¹⁹ The high pressure and temperature environment during the coalification process may produce similar effects with those of the thermal or hydrothermal treatment, thus carbonizing the buried organics into kinds of carbon based nanomaterials, especially the GQDs. Then over many millions of years, with the continuing effects of temperature and pressure, the hydrogen and oxygen contents were decreased while the carbon content was increased. Meanwhile, those tiny GQDs were aggregated and further formed bigger carbon structures, including GO, carbon nanocrystals, inordinate graphite clumps and so on.

Conclusions

S-GQDs with an average height of about 0.5 nm and an average plane dimension of about 10 nm were obtained from coal by a simple chemical oxidation and centrifugation method. The obtained S-GQDs show excitation-dependent FL and excellent ECL properties. The production yield of S-GQDs was revealed to be obviously dependent on the rank of coal. It decreased from 56.30% to 14.66% when the rank of the six investigated coals was gradually increased. Besides S-GQDs, some other CNMs such as GO, CQDs, agglomerate GQDs and agglomerate CQDs could also be found in coal, implying that coal may also be used to prepare these CNMs.

Acknowledgements

This study was financially supported by National Natural Science Foundation of China (21375020, 21305017), Program for New Century Excellent Talents in Chinese University (NCET-10-0019), National Basic Research Program of China (2010CB732400), and the Program for Changjiang Scholars and Innovative Research Team in University (No. IRT1116).

Notes and references

Ministry of Education Key Laboratory of Analysis and Detection for Food Safety, Fujian Provincial Key Laboratory of Analysis and Detection for Food Safety, and Department of Chemistry, Fuzhou University, Fujian 350108, China. Fax: +86-591-22866137; Tel: +86-591-22866137; E-mail: y.w.chi@fzu.edu.cn
Electronic Supplementary Information (ESI) available: Elemental analysis results of coal samples, FTIR spectra of Coal_A and Coal_B, ECL responses of Coal_A/S₂O₈²⁻. See DOI: 10.1039/b000000x/

- H. W. Kroto, J. R. Heath, S. C. O'Brien, R. F. Curl and R. E. Smalley, *Nature*, 1985, **318**, 162–163.
- S. Iijima, *Nature*, 1991, **354**, 56–58.
- T. Braun, A. P. Schubert and R. N. Kostoff, *Chem. Rev.*, 2000, **100**, 23–37.
- L. Hu, D. S. Hecht and G. Gruner, *Chem. Rev.*, 2010, **110**, 5790–5844.
- Y. Zhu, S. Murali, W. Cai, X. Lim, J. W. Suk, J. R. Potts and R. S. Ruoff, *Adv. Mater.*, 2010, **22**, 3906–3924.
- G. Eda, Y. Lin, C. Mattevi, H. Yamaguchi, H. Chen, I. Chen, C. Chen and M. Chhowalla, *Adv. Mater.*, 2010, **22**, 505–509.
- K. P. Loh, Q. Bao, G. Eda and M. Chhowalla, *Nat. Chem.* 2010, **2**, 1015–1024.
- F. F. Fan, S. Park, Y. Zhu, R. S. Ruoff and A. J. Bard, *J. Am. Chem. Soc.* 2009, **131**, 937–939.
- Y. Zhu, S. Murali, W. Cai, X. Li, J. W. Suk, J. R. Potts and R. S. Ruoff, *Adv. Mater.*, 2010, **22**, 3906–3924.
- M. J. Allen, V. C. Tung and R. B. Kaner, *Adv. Mater.*, 2010, **110**, 132–145.
- Y. P. Sun, B. Zhou, Y. Lin, W. Wang, K. A. S. Fernando, P. Pathak, M. J. Meziani, B. A. Harruff, X. Wang, H. F. Wang, P. J. G. Luo, H. Yang, M. E. Kose, B. L. Chen, L. M. Veca and S. Y. Xie, *J. Am. Chem. Soc.* 2006, **128**, 7756–7757.
- L. A. Ponomarenko, F. Schedin, M. I. Katsnelson, R. Yang, E. W. Hill, K. S. Novoselov and A. K. Geim, *Science* 2008, **320**, 356–358.
- S. N. Baker and G. A. Baker, *Angew. Chem. Int. Ed.* 2010, **49**, 6726–6744.
- Z. Zhang, J. Zhang, N. Chen and L. Qu, *Energy Environ. Sci.*, 2012, **5**, 8869–8890.
- J. Shen, Y. Zhu, X. Yang and C. Li, *Chem. Commun.* 2012, **48**, 3686–3699.
- W. Lu, X. Qin, S. Liu, G. Chang, Y. Zhang, Y. Luo, A. M. Asiri, A. O. Al-Youbi and X. Sun, *Anal. Chem.* 2012, **84**, 5351–5357.
- S. Liu, J. Tian, L. Wang, Y. Zhang, X. Qin, Y. Luo, A. M. Asiri, A. O. Al-Youbi and X. Sun, *Adv. Mater.*, 2012, **24**, 2037–2041.
- Y. Dong, H. Pang, C. Guo, J. Shao, Y. Chi, C. M. Li and T. Yu, *Angew. Chem. Int. Ed.* 2013, **52**, 7800–7804.
- Y. Dong, J. Shao, C. Chen, H. Li, R. Wang, Y. Chi, X. Lin and G. Chen, *Carbon* 2012, **50**, 4738–4743.
- H. Zhu, X. Wang, Y. Li, Z. Wang, F. Yang and X. Yang, *Chem. Commun.* 2009, 5118–5120.
- H. Peng and J. Travas-Sejdic, *Chem. Mater.* 2009, **21**, 5563–5565.
- H. Li, X. He, Y. Liu, H. Huang, S. Lian, S. Lee and Z. Kang, *Carbon* 2011, **49**, 605–609.
- X. Yan, X. Cui and L. Li, *J. Am. Chem. Soc.* 2010, **132**, 5944–5945.
- R. Liu, D. Wu, X. Feng and K. Müllen, *J. Am. Chem. Soc.* 2011, **133**, 15221–15223.
- S. Sahu, B. Behera, T. K. Maiti and S. Mohapatra, *Chem. Commun.* 2012,

- 48, 8835–8837.
- 26 C. Zhu, J. Zhai and S. Dong, *Chem. Commun.* 2012, **48**, 9367–9369.
- 27 L. Lin and S. Zhang, *Chem. Commun.* 2012, **48**, 10177–10179.
- 28 Y. Li, Y. Hu, Y. Zhao, G. Shi, L. Deng, Y. Hou and L. Qu, *Adv. Mater.* 2011, **22**, 776–780.
- 29 D. Pan, J. Zhang, Z. Li and M. Wu, *Adv. Mater.* 2010, **22**, 734–738.
- 30 S. Zhu, J. Zhang, C. Qiao, S. Tang, Y. Li, W. Yuan, B. Li, L. Tian, F. Liu, R. Hu, H. Gao, H. Wei, H. Zhang, H. Sun and B. Yang *Chem. Commun.* 2011, **47**, 6858–6860.
- 31 Y. Dong, H. Pang, S. Ren, C. Chen, Y. Chi and T. Yu, *Carbon* 2013, **64**, 245–251.
- 32 Y. Dong, N. Zhou, X. Lin, J. Lin, Y. Chi, G. Chen, *Chem. Mater.* 2010, **22**, 5895–5899.
- 33 J. Peng, W. Gao, B. K. Gupta, Z. Liu, R. Romero-Aburto, L. Ge, L. Song, L. B. Alemany, X. Zhan, G. Gao, S. A. Vithayathil, B. A. Kaiparettu, A. A. Marti, T. Hayashi, J. Zhu and P. M. Ajayan. *Nano Lett.* 2012, **12**, 844–849.
- 34 Y. Dong, Q. Chen, X. Zheng, L. Gao, Z. Cui, H. Yang, C. Guo, Y. Chi and C. Li, *J. Mater. Chem.* 2012, **22**, 8764–8766.
- 35 A. B. Bourlinos, A. Stassinopoulos, D. Anglos, R. Zboril, M. Karakassides, E. P. Giannelis, *Small* 2008; **4**, 455–458.
- 36 X. Y. Yang, X. Dou, A. Rouhanipour, L. J. Zhi, H. J. Rader, K. Müllen, *J. Am. Chem. Soc.* 2008, **130**, 4216–4217.